



Cite this: *Chem. Sci.*, 2025, **16**, 2690

All publication charges for this article have been paid for by the Royal Society of Chemistry

Received 13th November 2024
Accepted 22nd November 2024

DOI: 10.1039/d4sc07681h
rsc.li/chemical-science

Introduction

Phenyl rings, as readily available building blocks, undergo dearomatic functionalization reactions to yield a variety of valuable skeletons that have garnered significant attention in organic synthesis.^{1–3} The chemodivergent dual-functionalization dearomatization strategy not only introduces two additional functional groups into the cyclic system but also substantially enhances the structural diversity of three-dimensional molecules.⁴ By leveraging an aromaticity disassembly-reconstruction process,⁵ peripheral editing of the benzene ring can be further achieved.⁶

Compared to the traditional two-electron pathway for dearomatization of phenyl rings,^{7–9} radical-mediated dearomatizations are of interest as they tend to use mild conditions that overcome the unfavorable thermodynamics, especially for non-activated phenyl rings.^{10–12} The transience of the cyclohexadienyl radical (CHDR) intermediate during the dearomatization event, along with its high reactivity, are key factors for

subsequent transformations. The radical-polar crossover (RPC)^{13–15} mechanism is well established for intercepting these radical species, leading to the irreversible generation of the corresponding ionic intermediates (Scheme 1A, upper left). Despite significant advances and their great potential, RPC strategies still have limited applications for diverse post-functionalization. For example, reductive RPC produces carbanion species, which primarily undergo protonation accompanied by few functionalizations,^{16–24} while oxidative RPC usually results in diones *via* cation intermediates.^{25–31} Recently, a combination of CHDR and palladium catalyst to form the cyclohexadienyl Pd(II) species³² may be a potential direction for expanding CHDR chemistry (Scheme 1A, lower left). Nevertheless, it is still highly desirable to continue to seek efficient transformations using CHDRs.

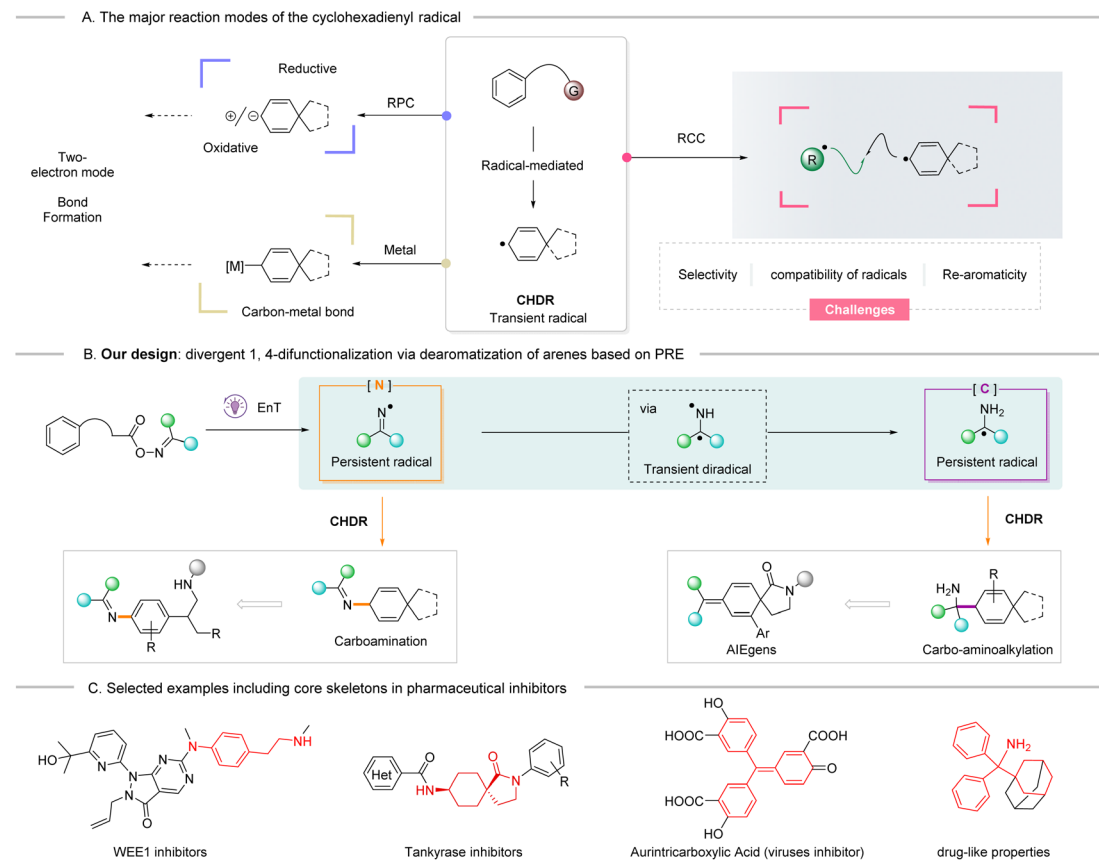
The radical cross-coupling (RCC) strategy has emerged as a powerful tool for difunctionalization of alkenes and other unsaturated systems.^{33,34} We envisioned that this methodology can be implemented during the dearomatic process of a non-activated phenyl ring (masked cyclic triene), namely, the CHDR is terminated by another radical, to greatly expand the dearomatization chemical library (Scheme 1A, right). It is intriguing to mention that some intramolecular radical cyclo-addition strategies have already been established.^{35–39} However, several challenges should be highlighted, especially in intermolecular processes, such as chemo-/regioselectivity, reactivity and compatibility of the radical species, as well as undesirable

Key Laboratory of Functional Molecular Engineering of Guangdong Province, School of Chemistry and Chemical Engineering, South China University of Technology (SCUT), Guangzhou 510640, China

† This article is dedicated to professor Yulin Wu to express our deep memory.

‡ Electronic supplementary information (ESI) available: Experimental details and characterization of all compounds, and copies of ¹H, ¹³C and ¹⁹F NMR spectra. See DOI: <https://doi.org/10.1039/d4sc07681h>





Scheme 1 (A) Representative reaction modes of the cyclohexadienyl radical; (B) designed strategy and this work: divergent difunctionalization through dearomatic radical-cross coupling of phenyl rings based on persistent radical effect (PRE); (C) selected examples including target skeletons in value-added molecules.

side reactions.^{40–42} Encouragingly, this pathway might be facilitated by leveraging the persistent radical effect (PRE), which relies on a kinetic mechanism to govern the RCC process. In this process two different radicals with different lifetimes are simultaneously generated.^{43–45} Therefore, potential radical partners should possess persistence, stability, and a low rate of homocoupling.

With the above concept in mind, the persistent diphenyliminyl radical was considered an excellent choice as it not only efficiently undergoes heterocoupling, but it is also easily obtained from the homolytic cleavage of oxime esters *via* visible-light mediated triplet-triplet EnT.^{46–58} On the other hand, it was hypothesized that another persistent C-centered α -amino radical could be generated *in situ* from the diphenyliminyl radical through HAT/EnT/second HAT cascade under tunable conditions within the dearomatic event.⁵⁹ Herein, as part of our ongoing research into the dearomatic difunctionalization of arenes,^{32,38,60} we report a chemodivergent RCC strategy that utilizes the PRE to recombine the cyclohexadienyl radical with the diphenyliminyl N-radical which ultimately leads to the dearomatic carboamination, or to recombine the cyclohexadienyl radical with the α -amino C-radical generated from the same substrate, which ultimately leads to carbo-aminoalkylation of non-activated phenyl rings (Scheme 1B).

All these core skeletons are versatile scaffolds commonly employed in pharmaceutical molecules (Scheme 1C).

Results and discussion

N-benzoyl propanoic O-oxime **1-1** was used as the model substrate to investigate this chemodivergent reaction. **1-1** can generate a persistent iminyl radical and a transient CHDR intermediate through an intramolecular dearomatic event by the EnT catalysts cascade. The desired RCC products were successfully obtained under the screening conditions outlined in Table 1. Initially the reaction was carried out in presence of 9H-thioxanthen-9-one (TXT) with MeCN as the solvent at room temperature providing only a 34% yield of **2-1** (entry 1). Through careful analysis of the reaction products (see ESI‡ for details), we believed that additional supplementation of the iminyl radical precursor would improve the C–N bond formation process. Subsequently, dioxime oxalate **A-1** was chosen as the additional iminyl radical source to further screen solvents. As expected, a significantly increased **2-1** yield was observed (60%) when MeCN was the solvent (entry 4). Additionally, the mixed solvent (MeCN/EA = 2/1, *v/v*) had a slightly positive effect (entry 5). THF or DMF⁶¹ as potential HAT precursors are commonly employed in the formation of chemical bonds.⁶² These solvents



Table 1 Optimization of reaction conditions^a

Entry	Conditions			Yield ^b (%)		
	Solvent	Additives	Variation	2-1	cis/trans	3-1
1	MeCN	—	PC-I	34	1 : 3.0	0
2	DCE	A-1	PC-I	35	1 : 2.6	0
3	EA	A-1	PC-I	39	1 : 3.6	0
4	MeCN	A-1	PC-I	60	1 : 2.5	0
5	MeCN/EA (2/1, v/v)	A-1	PC-I	62	1 : 2.4	0
6	MeCN/EA (2/1, v/v)	A-1	Other PC/no $h\nu$ or PC	0		0
7	THF	A-1	PC-I	33	1 : 2.9	0
8	DMF	A-1	PC-I	24	1 : 2.7	0
9	EA	A-2	PC-I	0	2.0 : 1	25
10	DMPU	A-1	PC-I	0	1.7 : 1	37
11	DMPU/EA (1/1, v/v)	A-1	PC-I	0	1.8 : 1	55
12	DMPU/EA (1/1, v/v)	A-3	PC-I	0	1.8 : 1	60
13 ^c	DMPU/EA (1/1, v/v)	A-3	PC-I	0	1.9 : 1	69
14	DMPU/EA (1/1, v/v)	A-3	Other PC/no $h\nu$ or PC	0		0

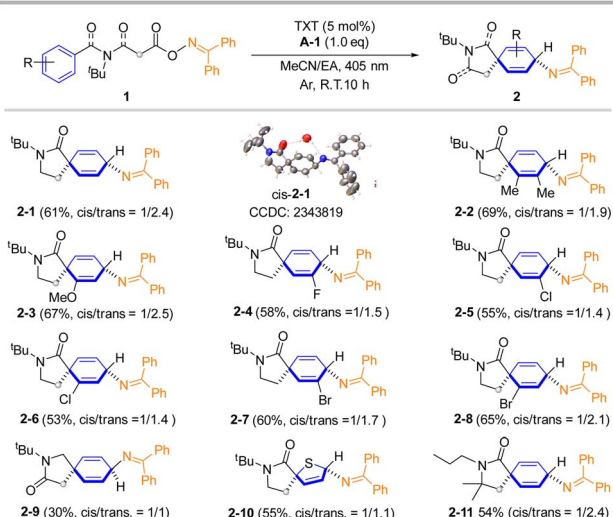
^a Standard conditions: the reactions were carried out under argon using **1-1** (0.1 mmol), Additive (1.0 equiv.), PC (5 mol%), Solvents for **2-1** (0.033 M), Solvents for **3-1** (0.05 M) at room temperature for 10 h. ^b The yield of **2-1** and **3-1** were based on ¹H NMR analysis of the crude product using CH₂Br₂ as the internal standard. ^c Additive (2.0 equiv.). EA = ethyl acetate, DMPU = 1,3-dimethyltetrahydropyrimidin-2(1*H*)-one.

were initially evaluated in the presence of **A-1** to generate the desired product **3-1**. Unfortunately, these experiments failed to produce **3-1**, with the reaction favoring the formation of product **2-1** in low yields (entries 7 and 8). Notably, when the reaction was conducted in the presence of γ -terpinene (**A-2**)⁶³ in EA (entry 9), the desired product **3-1** was afforded in a 25% yield, along with approximately a 15% yield of the CHDR homodimer. Gratifyingly, DMPU⁶⁴ exhibited a significant enhancing effect (entry 10), especially in combination with EA as the mixed solvent, affording product **3-1** in 55% yield (entry 11). Benzo-phenone imine (**A-3**), a simpler additive, increased the yield of product **3-1** to 60% (entry 12). Furthermore, increasing the loading of **A-3** from 1.0 to 2.0 equiv. resulted in a significant reaction efficiency improvement (entry 13) giving the target product **3-1** in 69% yield. Control experiments confirmed that both photoirradiation and the TXT catalyst were necessary for all the desired reactions (entries 6 and 14). Nevertheless, we recognized that the low *cis/trans*-selectivity for both transformations might arise from lower steric control during the radical–radical recombination events. Additionally, the increased proportion of *cis*-selectivity in carbo-aminoalkylation

may be ascribed to the presence of intramolecular hydrogen bonding.

With the optimal conditions in hand, the scope of the carboamination for non-activated phenyl substrates was investigated. As summarized in Scheme 2, various O-oxime esters derived from benzamidopropanoic acids afford the corresponding spiro-cyclohexadienyl imines in moderate to good yields. X-ray crystallographic analysis revealed the major product to be **2-1** (*trans*), with the amide carbonyl and imine moieties positioned opposite each other.⁶⁵ The minor product, **2-1** (*cis*) was also identified. Compared to the unsubstituted phenyl product **2-1** (61% yield), the heterocoupling process showed a slight improvement in yields when substituents were present at the ortho- or meta-positions of the starting materials. Products **2-2** and **2-3** were obtained in 69% and 67% yield. Notably, it is easy to obtain cyclohexadienyl amine from **2** in the presence of weak acid conditions (see ESI† for detail). On the other hand, the electron-deficient groups such as F, Cl, Br on the 2- or 3-position of benzene ring were also compatible, giving corresponding products in 53% to 65% yields (**2-4** to **2-8**). The *N*-benzyl-derived malonate O-oxime ester also provided the

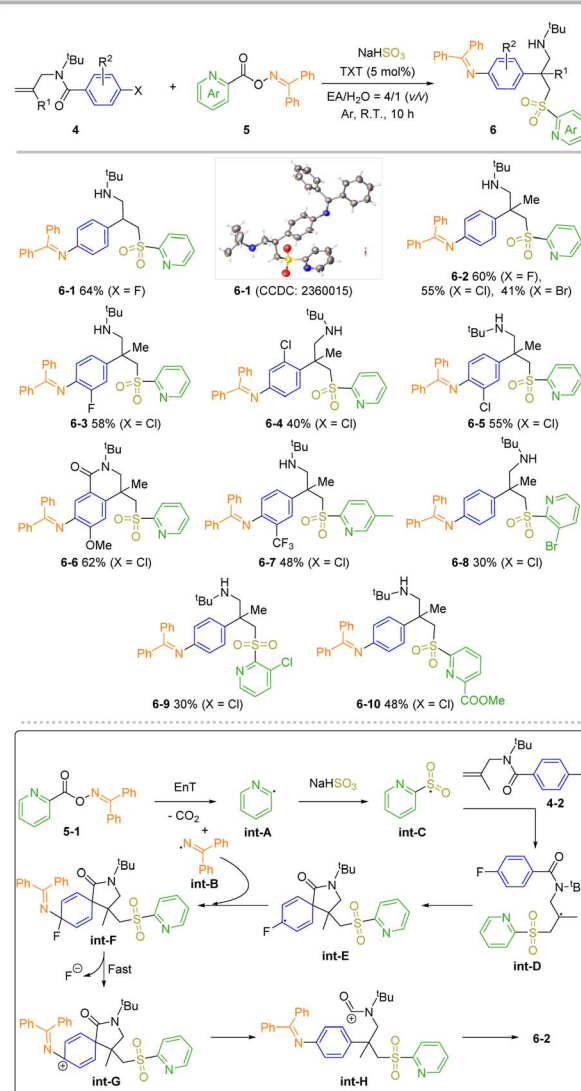




Scheme 2 Substrate scopes for carboamination. Reaction conditions: O-oxime ester **1** (0.2 mmol), **A-1** (0.2 mmol, 1.0 equiv.), TXT (5 mol%) in 6 mL of MeCN/EA (0.033 M, v/v = 2/1) under Ar atmosphere at room temperature and irradiated with visible LEDs (2 × 15 W, 405 nm) for 10 h. Isolated yields are reported as the average of four experiments.

dearomatic product **2-9**, albeit with an apparent decrease in yield, possibly due to the C–N bond is susceptible to hydrolysis, whereas steric bulk on the cyclohexadienyl amine can stabilize the C–N bond. This transformation also proceeded well when the reaction was performed on a starting material containing a thiophene ring, affording product **2-10** in a 55% yield. When *N*-propyl was used, the reaction yielded product **2-11** in 54% yield. It should be noted that the Thorpe–Ingold effect enhanced the dearomatic event while there was minimal steric hindrance from the *N*-protected group (**2-11**). Notably, dearomatic carboamination is completely inhibited by a substituent at the para-position of the phenyl ring or the 5-position of the thiophene ring (see ESI† for details).

To make the method more useful and develop the product for new and diverse applications, we envisioned that the amine-substituted benzene ring can be achieved through a rearomatic strategy,⁶⁶ yielding 4-(2-aminoethyl)aniline derivatives. These derivatives are crucial building blocks for pharmaceuticals and liquid crystal materials. Traditionally, the pathway for introducing an amino group on the phenyl ring involves challenging nitration and reduction steps. Upon treatment of 4-bromobenzoyl-linked O-oxime ester under the standard carboamination conditions, no formation of rearomatic product was observed. Interestingly, when this process was switched to an intermolecular approach, namely using **4** and **5** as starting materials, the desired product **6** was successfully obtained under modified conditions (Scheme 3). To probe this transformation's functional group tolerance, this reaction was carried with **4-1** ($X = F$) as the substrate. The desired product **6-1** was obtained in 64% yield, and its configuration confirmed through X-ray crystallographic analysis.⁶⁷ It was found that the steric hindrance from the β -position of allyl (**4**, $R^1 = Me$) is compatible, giving all-carbon quaternary center^{68,69} products in



Scheme 3 Substrate scopes for transient dearomatization and plausible mechanism. Reaction conditions: *N*-allyl-*N*-(tert-butyl)benzamide **4** (0.2 mmol), O-oxime ester **5** (0.34 mmol, 1.7 equiv), NaHSO₃ (0.6 mmol, 3.0 equiv), TXT (5 mol%) in 5 mL of EA/H₂O (v/v = 4/1) under Ar atmosphere at room temperature and irradiated with visible LEDs (2 × 15 W, 405 nm) for 10 h. Isolated yields are reported as the average of two experiments.

moderate to good yields (**6-2**, 41% to 60% yields). The effect of different halogens ($X = F, Cl, Br$) was also investigated. Interestingly, a decrease in the yield was observed with increasing atomic radius of the halogen. Next, several substrates **4** with different substitutions on the phenyl ring were examined. They produced the corresponding all-carbon quaternary center products in good yields (**6-3** to **6-7**). Significantly, rearomatic cyclization product **6-6** was achieved in 62% yield, this outcome strongly indicates that a Friedel–Crafts cyclization occurred between the electron-rich phenyl ring and the amide carbocation during the cascade process. Finally, a range of O-picolinoyl oxime substrates **5** bearing different substitutions on the pyridyl ring were investigated, and the corresponding all-carbon

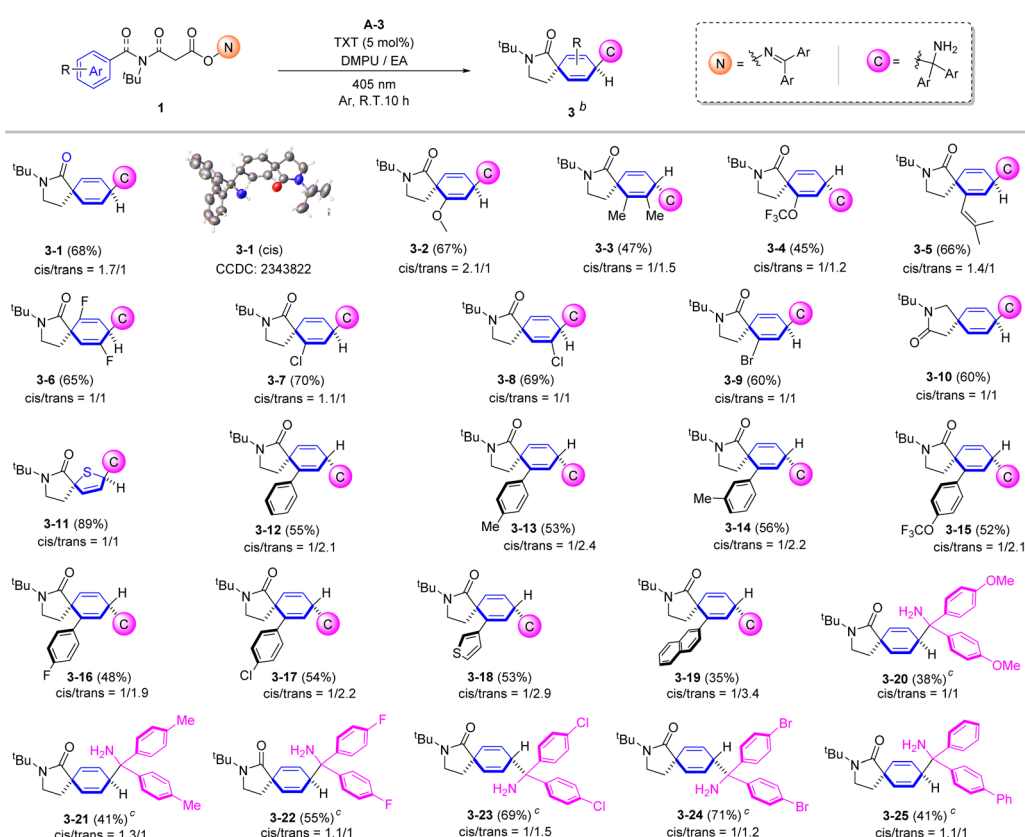


quaternary products (**6-7** to **6-10**) were obtained. Note that the yields of products decreased when there was steric hindrance at the C3 position of the pyridyl ring (30% yields for both **6-8** and **6-9**).

Based on the experiment outcomes, and our recently reported results,⁶⁶ a plausible reaction mechanism for this transient dearomatization process is proposed in Scheme 3 (bottom). N–O bond cleavage occurs in the triplet state of **5-1** (generated by EnT process with excited TXT), followed by the release of CO₂ to yield **int-A** and **int-B**. **int-A** quickly reacts with SO₂ to form a sulfonyl radical **int-C**, which then affords the **int-D** through radical addition with alkene **4-2**.^{70,71} The key intermediate, **int-F** forms *via* a radical-induced dearomatization/RCC process cascade from **int-D**. Then, a rapid dehalogenation process takes place *in situ* to yield **int-G**, which provides the 4-(2-aminoethyl)-aniline derivatives **6-2** through the rearomatization cation **int-H**.⁷² When a more electron-rich phenyl ring is involved, a Friedel–Crafts cyclization event will take place.

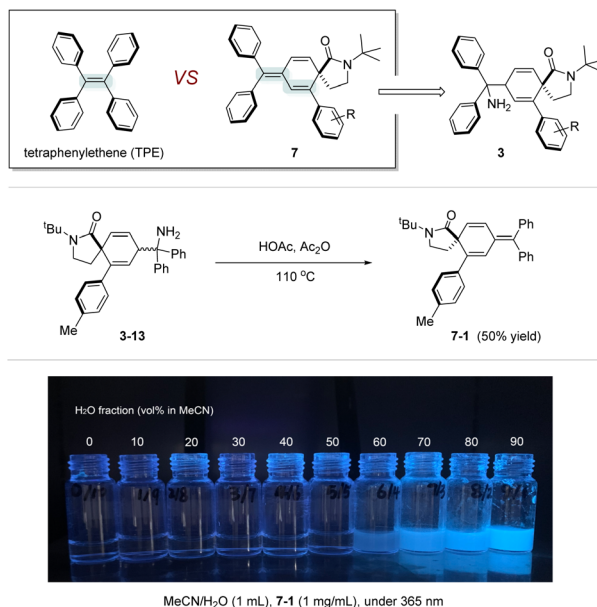
Next, an investigation into the substrate's compatibility for the carbo-aminoalkylation reaction was conducted and the results summarized in Scheme 4. The standard product **3-1** was obtained in 68% yield (*cis/trans* = 1.7/1). X-ray crystallographic analysis confirmed a *cis* configuration for the major diastereomer which exhibits low polarity.⁷³ A large variety of

substituents on the phenyl ring gave the corresponding spiro carbo-aminoalkylation products (**3-2** to **3-9**) in moderate to good yields. Notably, different electronic properties such as methoxy (**3-2**), 2,3-dimethyl (**3-3**), trifluoromethoxy (**3-4**), isobut enyl (**3-5**) and halides (**3-6** to **3-9**) were well tolerated. In addition, a malonic acid derived O-oxime reagent afforded product **3-10** in 60% yield, showing the formal transposition of the carbonyl group relative to the standard product. Gratifyingly, as mentioned earlier, when employing a thiophene ring substrate, product **3-11** was obtained in excellent yield (up to 89%). *ortho*-Aryl biphenyl O-oxime ester substrates bearing a broad range of substituents on the aryl position, including methyl (**3-13** and **3-14**), trifluoromethoxy (**3-15**), and halides (**3-16** and **3-17**), underwent the reaction to provide the desired products in moderate yields (48% to 56%). Additionally, this reaction tolerated other aryl substituents at the *ortho*-position, such as 3-thiophenyl (**3-18**) and 2-naphthalenyl (**3-19**). However, the yield was significantly affected by the steric hindrance of the aryl moiety, with bulkier substituents leading to lower yields. Notably, the reaction exhibited a remarkable preference for the trans configuration due to the steric hindrance imposed by the *ortho*-aryl group. Furthermore, the electronic effect of the symmetrical benzene rings on the diphenyl imine radical was studied. Increasing product yield was observed as the



Scheme 4 Substrate scope for carbo-aminoalkylation. Reaction conditions: ^a O-oxime ester **1** (0.2 mmol), **A-3** (0.4 mmol, 2.0 equiv.), TXT (5 mol%) in 4 mL of DMPU/EA (0.05 M, v/v = 1/1) under Ar at room temperature and irradiated with visible LEDs (2 x 15 W, 405 nm) for 10 h. Isolated yields are reported as the average of four experiments. ^b Major products were visualized. ^c The corresponding imine additive was used instead of **A-3**.





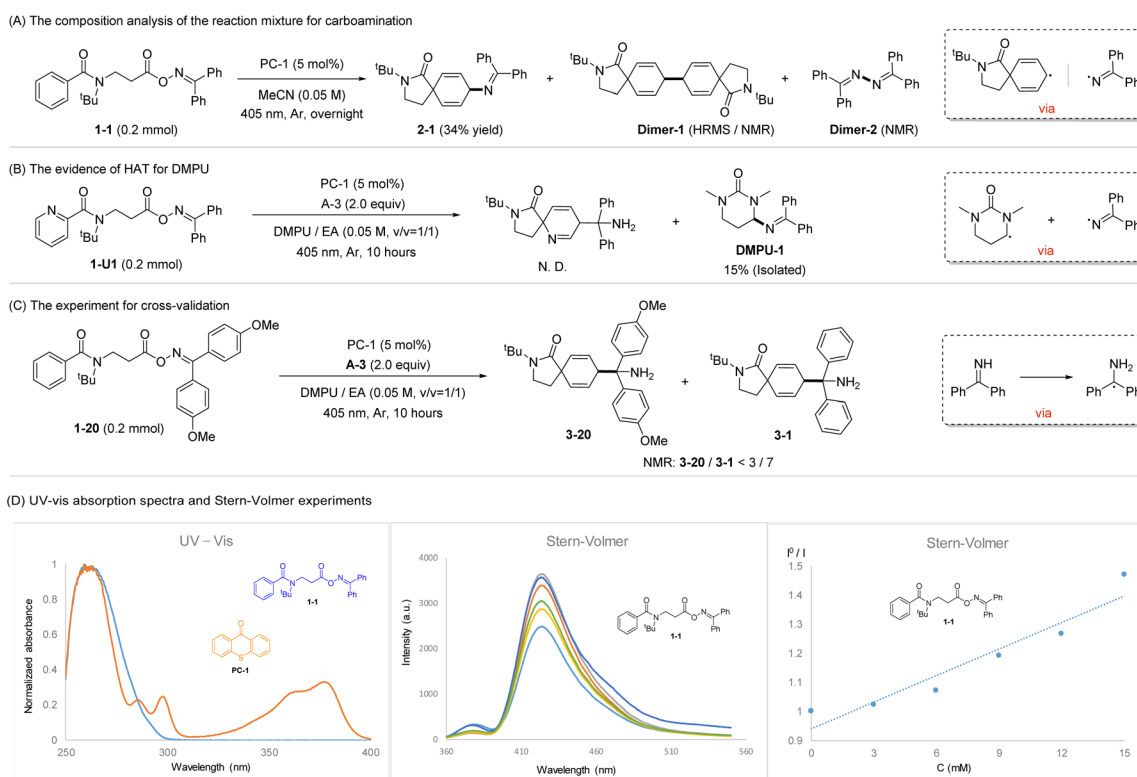
Scheme 5 The synthesis of a novel AIogens structure and fluorescence experiment. Reaction conditions: 3-13 (0.3 mmol), in 3 mL of HOAc/Ac₂O (v/v = 1/2) under Ar atmosphere at 110 °C for 20 h. Isolated yield is reported.

substituents on the diphenyl ring evolved from electron-donating methoxy (3-20, 38% yield) and methyl (3-21, 41% yield) groups to electron-withdrawing fluoro (3-22, 55% yield), chloro (3-23, 69% yield), and bromo (3-24, 71% yield) groups.

This observation underscores the profound impact of electronic effects on the outcomes of the reaction. Finally, the reaction successfully incorporated a non-symmetric diphenyl imine radical, affording product 3-25 in a moderate 41% yield.

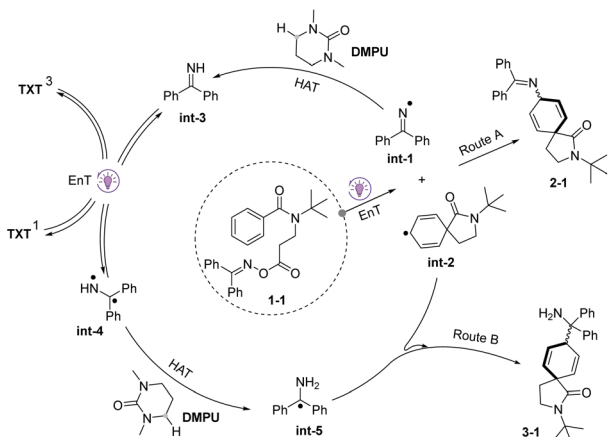
Inspired by the well-studied tetraphenylethylene (TPE) AIE materials, we realized that the conjugated triphenylcyclohexadiene product 7 (Scheme 5), likely formed *via* NH₃ elimination from 3, is expected to exhibit a similar AIE effect. To investigate this hypothesis further, a new molecule, 7-1, was synthesized. Its fluorescence image ($\lambda_{\text{irr}} = 365$ nm) at different compositions is shown in Scheme 5 (bottom) and supports the AIE property.

To gain insights into the reaction mechanism, a series of control experiments were conducted under specific conditions, and the corresponding results are provided in Scheme 6. Careful analysis of the initial reaction mixture by HRMS and NMR shows the desired product 2-1 was present along with dimer byproducts Dimer-1 and Dimer-2 (Scheme 6A). This observation suggests the involvement of the cyclohexadienyl and the iminyl radical as reaction intermediates. Switching from benzamide O-oxime ester to picolinamide O-oxime ester did not yield the desired product, however, the reaction surprisingly afforded a key intermediate DMPU-1 in 15% yield (Scheme 6B). This result strongly implies a HAT process under the standard conditions, potentially with DMPU acting as the hydrogen atom donor or a mediator in the process. To validate our hypothesis, a cross-validation experiment, reacting 1-20 with A-3 under standard conditions, was performed. NMR analysis of the inseparable reaction products revealed 3-1



Scheme 6 Control experiments.





Scheme 7 Plausible mechanism.

as the major component and **3-20** as a minor component (Scheme 6C). This finding illustrates that the α -amino carbon-centered radical arises from the transformation of **A-3** *via* a triplet EnT/HAT cascade process. UV-vis characterization of **1-1** and **PC-1** revealed that **1-1** cannot be directly excited by visible-light. Furthermore, the Stern–Volmer experiments elucidated that an EnT process between **1-1** and excited-state **PC-1** (Scheme 6D).

Based on the above experimental results, a proposed photocatalytic pathway for the chemodivergent radical cross-coupling is outlined in Scheme 7. Initially, O-oxime ester **1-1** undergoes excitation *via* an EnT process, followed by N–O bond homolysis of triplet state **1-1***. This event, coupled with releasing CO_2 and an intramolecular dearomatization process, leads to the formation of the *N*-centered radical **int-1** and the CHDR **int-2**. These two radicals readily couple together, leading to the formation of product **2-1** (route A). However, the presence of a suitable HAT donor, such as DMPU, disrupts this established coupling process, leading to the formation of imine **int-3** *via* an alternative pathway. Subsequently, imine **int-3** can be directly excited by excited TXT to generate its triplet state (**int-4**),⁷⁴ followed by a second HAT process with DMPU, yielding **int-5**. Ultimately, the radical–radical cross-coupling between **int-2** and **int-5** affords product **3-1** (route B), forming a new $\text{C}(\text{sp}^3)\text{–C}(\text{sp}^3)$ bond instead of the above $\text{C}(\text{sp}^3)\text{–N}(\text{sp}^2)$ bond.

Conclusions

In summary, an energy transfer catalysis strategy was developed to enable chemodivergent dearomatization of benzene rings. This strategy harnesses the PRE to accomplish both carboamination and carbo-aminoalkylation through RCC. Employing this protocol, four structurally distinct molecular frameworks were synthesized *via* divergent pathways. We believe this discovery represents a groundbreaking advancement in C–C bond formation by utilizing O-oxime esters. It marks a significant departure from the traditional paradigm of C–N bond formation and holds immense potential for expanding the chemical library.

Data availability

Supporting data or code have been included in the article's ESI[†].

Author contributions

This work was conceptualized by G. Z. and prof. B. Y. experimentation was performed by G. Z. and D. G. The first draft of the manuscript was prepared by G. Z. and the final version was edited and revised by prof. B. Y. and prof. H. J.

Conflicts of interest

There are no conflicts to declare.

Acknowledgements

This work was financially supported by the Natural Science Foundation of Guangdong Province (no. 2023A1515010771). We also thank Prof. Honggen Wang (Sun Yat-Sen University) and Prof. Pengju Feng (Jinan University) for helpful discussions.

Notes and references

- 1 S. P. Roche and J. A. Porco, Dearomatization Strategies in the Synthesis of Complex Natural Products, *Angew. Chem., Int. Ed.*, 2011, **50**, 4068–4093.
- 2 W. C. Wertjes, E. H. Southgate and D. Sarlah, Recent advances in chemical dearomatization of nonactivated arenes, *Chem. Soc. Rev.*, 2018, **47**, 7996–8017.
- 3 C. J. Huck and D. Sarlah, Shaping Molecular Landscapes: Recent Advances, Opportunities, and Challenges in Dearomatization, *Chem.*, 2020, **6**, 1589–1603.
- 4 I. P. Beletskaya, C. Nájera and M. Yus, Chemodivergent reactions, *Chem. Soc. Rev.*, 2020, **49**, 7101–7166.
- 5 L. Li, M. Yang, Q. He and R. Fan, Conversion of anilines to chiral benzylic amines *via* formal one-carbon insertion into aromatic C–N bonds, *Nat. Commun.*, 2020, **11**, 4805–4813.
- 6 Z. Fan, X. Chen, K. Tanaka, H. S. Park, N. Y. S. Lam, J. J. Wong, K. N. Houk and J.-Q. Yu, Molecular editing of aza-arene C–H bonds by distance, geometry and chirality, *Nature*, 2022, **610**, 87–93.
- 7 C. Zheng and S.-L. You, Advances in Catalytic Asymmetric Dearomatization, *ACS Cent. Sci.*, 2021, **7**, 432–444.
- 8 L. M. Comparini and M. Pineschi, Recent Progresses in the Catalytic Stereoselective Dearomatization of Pyridines, *Molecules*, 2023, **28**, 6186–6215.
- 9 M. Escolano, D. Gavíña, G. Alzuet-Piña, S. Díaz-Oltra, M. Sánchez-Roselló and C. d. Pozo, Recent Strategies in the Nucleophilic Dearomatization of Pyridines, Quinolines, and Isoquinolines, *Chem. Rev.*, 2024, **124**, 1122–1246.
- 10 M. Okumura and D. Sarlah, Visible-Light-Induced Dearomatizations, *Eur. J. Org. Chem.*, 2019, **2020**, 1259–1273.
- 11 Y.-Z. Cheng, Z. Feng, X. Zhang and S.-L. You, Visible-light induced dearomatization reactions, *Chem. Soc. Rev.*, 2022, **51**, 2145–2170.

12 D. H. Liu and J. Ma, Recent Advances in Dearomative Partial Reduction of Benzenoid Arenes, *Angew. Chem., Int. Ed.*, 2024, **63**, e202402819.

13 R. J. Wiles and G. A. Molander, Photoredox-Mediated Net-Neutral Radical/Polar Crossover Reactions, *Isr. J. Chem.*, 2020, **60**, 281–293.

14 S. Sharma, J. Singh and A. Sharma, Visible Light Assisted Radical-Polar/Polar-Radical Crossover Reactions in Organic Synthesis, *Adv. Synth. Catal.*, 2021, **363**, 3146–3169.

15 L. Pitzer, J. L. Schwarz and F. Glorius, Reductive radical-polar crossover: traditional electrophiles in modern radical reactions, *Chem. Sci.*, 2019, **10**, 8285–8291.

16 A. R. Flynn, K. A. McDaniel, M. E. Hughes, D. B. Vogt and N. T. Jui, Hydroarylation of Arenes *via* Reductive Radical-Polar Crossover, *J. Am. Chem. Soc.*, 2020, **142**, 9163–9168.

17 Y. Masuda, H. Tsuda and M. Murakami, Photoinduced Dearomatizing Three-Component Coupling of Arylphosphines, Alkenes, and Water, *Angew. Chem., Int. Ed.*, 2020, **60**, 3551–3555.

18 R. C. McAtee, E. A. Noten and C. R. J. Stephenson, Arene dearomatization through a catalytic N-centered radical cascade reaction, *Nat. Commun.*, 2020, **11**, 2528–2535.

19 H. Takeuchi, S. Inuki, K. Nakagawa, T. Kawabe, A. Ichimura, S. Oishi and H. Ohno, Total Synthesis of Zephycarinatines *via* Photocatalytic Reductive Radical ipso-Cyclization, *Angew. Chem., Int. Ed.*, 2020, **59**, 21210–21215.

20 Y. Gao, H. Wang, Z. Chi, L. Yang, C. Zhou and G. Li, Spirocyclative Remote Arylcarboxylation of Nonactivated Arenes with CO₂ *via* Visible-Light-Induced Reductive Dearomatization, *CCS Chem.*, 2022, **4**, 1565–1576.

21 Y. Wang, W.-Y. Zhang, Z.-L. Yu, C. Zheng and S.-L. You, SmI₂-mediated enantioselective reductive dearomatization of non-activated arenes, *Nat. Synth.*, 2022, **1**, 401–406.

22 Q.-Q. Zhao, J. Rehbein and O. Reiser, Thermoneutral synthesis of spiro-1,4-cyclohexadienes by visible-light-driven dearomatization of benzylmalonates, *Green Chem.*, 2022, **24**, 2772–2776.

23 C. Zhou, A. Shatskiy, A. Z. Temerdashev, M. D. Kärkäs and P. Dinér, Highly congested spiro-compounds *via* photoredox-mediated dearomative annulation cascade, *Commun. Chem.*, 2022, **5**, 92–99.

24 J. Li, A. Kumar and J. C. Lewis, Non-native Intramolecular Radical Cyclization Catalyzed by a B12-Dependent Enzyme**, *Angew. Chem., Int. Ed.*, 2023, **62**, e202312893.

25 S. Manna, P. K. Someswara Ashwathappa and K. R. Prabhu, Visible light-mediated ipso-annulation of activated alkynes: access to 3-alkylated spiro[4,5]-trienones, thiaspiro[4,5]-trienones and azaspiro[4,5]-trienones, *Chem. Commun.*, 2020, **56**, 13165–13168.

26 P. Chen, J. Xie, Z. Chen, B. Q. Xiong, Y. Liu, C. A. Yang and K. W. Tang, Visible-Light-Mediated Nitrogen-Centered Radical Strategy: Preparation of 3-Acylated Spiro[4,5]-trienones, *Adv. Synth. Catal.*, 2021, **363**, 4440–4446.

27 W. Dong, Y. Yuan, C. Liang, F. Wu, S. Zhang, X. Xie and Z. Zhang, Photocatalytic Radical Ortho-Dearomative Cyclization: Access to Spiro[4.5]deca-1,7,9-trien-6-ones, *J. Org. Chem.*, 2021, **86**, 3697–3705.

28 C. R. Azpilcueta-Nicolas, D. Meng, S. Edelmann and J. P. Lumb, Dearomatization of Biaryls through Polarity Mismatched Radical Spirocyclization, *Angew. Chem., Int. Ed.*, 2022, **62**, e202215422.

29 L. Li, Z.-W. Hou, P. Li and L. Wang, Electrochemical Dearomatizing Spirocyclization of Alkynes with Dimethyl 2-Benzylmalonates to Spiro[4.5]deca-trienones, *J. Org. Chem.*, 2022, **87**, 8697–8708.

30 M. Yang, J. Hua, H. Wang, T. Ma, C. Liu, W. He, N. Zhu, Y. Hu, Z. Fang and K. Guo, Photomediated Spirocyclization of N-Benzyl Propiolamide with N-Iodosuccinimide for Access to Azaspiro[4.5]deca-6,9-diene-3,8-dione, *J. Org. Chem.*, 2022, **87**, 8445–8457.

31 S. Samanta and D. Sarkar, Photoredox-Catalyzed Thiocyanative Cyclization of Biaryl Ynones to Thiocyanated Spiro[5.5]trienones: An External-Oxidant- and Transition-Metal-Free Approach, *ChemPhotoChem*, 2023, **7**, e202200335.

32 Q. Fan, K. Jiang, B. Liu, H. Jiang, X. Cao and B. Yin, Radical-Dearomative Generation of Cyclohexadienyl Pd(II) toward the 3D Transformation of Nonactivated Phenyl Rings, *Adv. Sci.*, 2023, **11**, 2307074–2307082.

33 J. Großkopf, T. Kratz, T. Rigotti and T. Bach, Enantioselective Photochemical Reactions Enabled by Triplet Energy Transfer, *Chem. Rev.*, 2021, **122**, 1626–1653.

34 L. Li, Q. Pang, B. Chen, Y. Liu, Y. Zhao, J. Wu, K. Ge, J. Shen and P. Zhang, A General Approach for the Synthesis of Cyanoisopropyl Bicyclo[1.1.1]pentane (BCP) Motifs by Energy Transfer Process, *Org. Lett.*, 2024, **26**, 7060–7065.

35 J. J. Ma, F. Strieth-Kalthoff, T. Dalton, M. Freitag, J. L. Schwarz, K. Bergander, C. Daniliuc and F. Glorius, Direct Dearomatization of Pyridines *via* an Energy-Transfer-Catalyzed Intramolecular [4+2] Cycloaddition, *Chem.*, 2019, **5**, 2854–2864.

36 J. Proessdorff, C. Jandl, T. Pickl and T. Bach, Arene Activation through Iminium Ions: Product Diversity from Intramolecular Photocycloaddition Reactions, *Angew. Chem., Int. Ed.*, 2022, **61**, e202208329.

37 M. Chiminelli, A. Serafino, D. Ruggeri, L. Marchiò, F. Bigi, R. Maggi, M. Malacria and G. Maestri, Visible-Light Promoted Intramolecular para-Cycloadditions on Simple Aromatics, *Angew. Chem., Int. Ed.*, 2023, **62**, e202216817.

38 G. Zhen, G. Zeng, F. Wang, X. Cao and B. Yin, Direct Construction of Fused/Bridged 3D Rings *via* Visible-Light Induced Dearomative Cycloaddition of Arenes, *Adv. Synth. Catal.*, 2023, **365**, 43–52.

39 M. Zhu, Y. J. Gao, X. L. Huang, M. Z. Li, C. Zheng and S. L. You, Photo-induced intramolecular dearomative [5+4] cycloaddition of arenes for the construction of highly strained medium-sized-rings, *Nat. Commun.*, 2024, **15**, 2462–2469.

40 B. Altundas, E. Alwedi, Z. H. Song, A. R. Gogoi, R. Dykstra, O. Gutierrez and F. F. Fleming, Dearomatization of aromatic asimic isocyanides to complex cyclohexadienes, *Nat. Commun.*, 2022, **13**, 6444–6451.

41 Y. Zhang, D. Yang, D. Lu and Y. Gong, Photoredox-Enabled Dearomatization of Protected Anilines: Access to



Cyclohexadienone Imines with Contiguous Quaternary Centers, *Org. Lett.*, 2023, **25**, 1320–1325.

42 P. F. Yuan, X. T. Huang, L. Long, T. Huang, C. L. Sun, W. Yu, L. Z. Wu, H. Chen and Q. Liu, Regioselective Dearomatative Amidoximation of Nonactivated Arenes Enabled by Photohomolytic Cleavage of N-nitrosamides, *Angew. Chem., Int. Ed.*, 2024, **63**, e202317968.

43 D. Leifert and A. Studer, The Persistent Radical Effect in Organic Synthesis, *Angew. Chem., Int. Ed.*, 2019, **59**, 74–108.

44 K. Yang, J. Liu, D. Fu, L. Niu, S.-J. Li and Y. Lan, A theoretical study of selective radical relay and coupling reactions for alkene difunctionalization, *Org. Chem. Front.*, 2023, **10**, 4336–4341.

45 H. Fischer, The Persistent Radical Effect: A Principle for Selective Radical Reactions and Living Radical Polymerizations, *Chem. Rev.*, 2001, **101**, 3581–3610.

46 V. K. Soni, S. Lee, J. Kang, Y. K. Moon, H. S. Hwang, Y. You and E. J. Cho, Reactivity Tuning for Radical–Radical Cross-Coupling *via* Selective Photocatalytic Energy Transfer: Access to Amine Building Blocks, *ACS Catal.*, 2019, **9**, 10454–10463.

47 T. Patra, P. Bellotti, F. Strieth-Kalthoff and F. Glorius, Photosensitized Intermolecular Carboimination of Alkenes through the Persistent Radical Effect, *Angew. Chem., Int. Ed.*, 2020, **59**, 3172–3177.

48 R. I. Rodríguez, M. Sicignano, M. J. García, R. G. Enríquez, S. Cabrera and J. Alemán, Taming photocatalysis in flow: easy and speedy preparation of α -aminoamide derivatives, *Green Chem.*, 2022, **24**, 6613–6618.

49 G. Tan, M. Das, H. Keum, P. Bellotti, C. Daniliuc and F. Glorius, Photochemical single-step synthesis of β -amino acid derivatives from alkenes and (hetero)arenes, *Nat. Chem.*, 2022, **14**, 1174–1184.

50 Y. Zheng, Z. J. Wang, Z. P. Ye, K. Tang, Z. Z. Xie, J. A. Xiao, H. Y. Xiang, K. Chen, X. Q. Chen and H. Yang, Regioselective Access to Vicinal Diamines by Metal-Free Photosensitized Amidylimination of Alkenes with Oxime Esters, *Angew. Chem., Int. Ed.*, 2022, **61**, e202212292.

51 L. Geniller, M. Taillefer, F. Jaroschik and A. Prieto, Photocatalyzed Amination of Alkyl Halides to Access Primary Amines, *J. Org. Chem.*, 2023, **89**, 656–664.

52 S.-S. Li, Y.-S. Jiang, X.-L. Luo, X. Ran, Y. Li, D. Wu, C.-X. Pan and P.-J. Xia, Photocatalytic vinyl radical-mediated multicomponent 1,4-/1,8-carboimination across alkynes and olefins/(hetero)arenes, *Sci. China:Chem.*, 2023, **67**, 558–567.

53 F. Paulus, C. Stein, C. Heusel, T. J. Stoffels, C. G. Daniliuc and F. Glorius, Three-Component Photochemical 1,2,5-Trifunctionalizations of Alkenes toward Densely Functionalized Lynchpins, *J. Am. Chem. Soc.*, 2023, **145**, 23814–23823.

54 G. Tan, F. Paulus, A. Petti, M.-A. Wiethoff, A. Lauer, C. Daniliuc and F. Glorius, Metal-free photosensitized radical relay 1,4-carboimination across two distinct olefins, *Chem. Sci.*, 2023, **14**, 2447–2454.

55 R. Laskar, S. Dutta, J. C. Spies, P. Mukherjee, Á. Rentería-Gómez, R. E. Thielemann, C. G. Daniliuc, O. Gutierrez and F. Glorius, γ -Amino Alcohols *via* Energy Transfer Enabled Brook Rearrangement, *J. Am. Chem. Soc.*, 2024, **146**, 10899–10907.

56 M.-J. Zheng, X.-K. Qi, C. Yang, L. Guo, Y. Zhao and W. Xia, Photoinduced amination of iodoalkanes enabled by bifunctional O-benzoyl oxime, *Org. Chem. Front.*, 2024, **11**, 1949–1954.

57 Y. Zhong, Z. Zhuang, X. Zhang, B. Xu and C. Yang, Difunctionalization of gem-difluoroalkenes for amination and heteroarylation *via* metal-free photocatalysis, *Chem. Commun.*, 2024, **60**, 4830–4833.

58 D. S. Lee, V. K. Soni and E. J. Cho, N–O Bond Activation by Energy Transfer Photocatalysis, *Acc. Chem. Res.*, 2022, **55**, 2526–2541.

59 M. C. Nicastri, D. Lehnher, Y.-h. Lam, D. A. DiRocco and T. Rovis, Synthesis of Sterically Hindered Primary Amines by Concurrent Tandem Photoredox Catalysis, *J. Am. Chem. Soc.*, 2020, **142**, 987–998.

60 G. Zeng, H. Luo, K. Jiang, J. Cai and B. Yin, Fully atom-economic access to spiro-cyclic skeletons through photoredox-induced hydrogen transfer/Giese addition/dearomative cyclization/protonation cascade, *Org. Chem. Front.*, 2024, **11**, 3165–3172.

61 L. Chen, K. Jiang, G. Zeng and B. Yin, Photoinduced Pd-Catalyzed Csp₂-H/Csp₃-H Dehydrocoupling Reaction Employing Polyhaloaromatics as the Dehydrogenating Agent, *Org. Lett.*, 2022, **24**, 9071–9075.

62 L. Capaldo, D. Ravelli and M. Fagnoni, Direct Photocatalyzed Hydrogen Atom Transfer (HAT) for Aliphatic C–H Bonds Elaboration, *Chem. Rev.*, 2021, **122**, 1875–1924.

63 D. H. Liu, K. Nagashima, H. Liang, X. L. Yue, Y. P. Chu, S. Chen and J. Ma, Chemoselective Quinoline and Isoquinoline Reduction by Energy Transfer Catalysis Enabled Hydrogen Atom Transfer, *Angew. Chem., Int. Ed.*, 2023, **62**, e202312203.

64 S. H. Cai, D. X. Wang, L. Ye, Z. Y. Liu, C. Feng and T. P. Loh, Pyrroline Synthesis *via* Visible-Light-Promoted Hydroimination of Unactivated Alkenes with N,N'-Dimethylpropylene Urea as H-Donor, *Adv. Synth. Catal.*, 2018, **360**, 1262–1266.

65 Deposition Number CCDC 2343819 *cis*-2-1 contains the supplementary crystallographic data for this paper. These data are provided free of charge by the joint Cambridge Crystallographic Data Centre and Fachinformationszentrum Karlsruhe Access Structures service.

66 J. Cai, G. Zeng, K. Jiang, H. Luo and B. Yin, Intramolecular Cobalt/Visible Light Cocatalyzed Reductive Coupling of Unactivated Arenes with Unactivated Alkenes, *Org. Lett.*, 2024, **26**, 327–331.

67 Deposition Number CCDC 2360015 6-1 contains the supplementary crystallographic data for this paper. These data are provided free of charge by the joint Cambridge Crystallographic Data Centre and Fachinformationszentrum Karlsruhe Access Structures service.



68 C. Hervieu, M. S. Kirillova, T. Suárez, M. Müller, E. Merino and C. Nevado, Asymmetric, visible light-mediated radical sulfinyl-Smiles rearrangement to access all-carbon quaternary stereocentres, *Nat. Chem.*, 2021, **13**, 327–334.

69 X.-c. Gan, B. Zhang, N. Dao, C. Bi, M. Pokle, L. Kan, M. R. Collins, C. C. Tyrol, P. N. Bolduc, M. Nicastri, Y. Kawamata, P. S. Baran and R. Shenvi, Carbon quaternization of redox active esters and olefins by decarboxylative coupling, *Science*, 2024, **384**, 113–118.

70 M. Chen, W. Sun, J. Yang, L. Yuan, J.-Q. Chen and J. Wu, Metal-free photosensitized aminosulfonylation of alkenes: a practical approach to β -amido sulfones, *Green Chem.*, 2023, **25**, 3857–3863.

71 X.-K. Qi, M.-J. Zheng, C. Yang, Y. Zhao, L. Guo and W. Xia, Metal-Free Amino(hetero)arylation and Aminosulfonylation of Alkenes Enabled by Photoinduced Energy Transfer, *J. Am. Chem. Soc.*, 2023, **145**, 16630–16641.

72 C. Faderl, S. Budde, G. Kachkovskiy, D. Rackl and O. Reisser, Visible Light-Mediated Decarboxylation Rearrangement Cascade of ω -Aryl-N-(acyloxy)phthalimides, *J. Org. Chem.*, 2018, **83**, 12192–12206.

73 Deposition Number CCDC 2343822 *cis*-3-1 contains the supplementary crystallographic data for this paper. These data are provided free of charge by the joint Cambridge Crystallographic Data Centre and Fachinformationszentrum Karlsruhe Access Structures service.

74 S. K. Ghosh, L. He, Z. Tang and R. J. Comito, Selective and Functional-Group-Tolerant Photoalkylation of Imines by Energy-Transfer Photocatalysis, *J. Org. Chem.*, 2023, **88**, 15209–15217.

